Interconnect Characterization Using Time-Domain Reflectometry

Steven D. Corey and Andrew T. Yang

Abstract—**An approach is presented for modeling board-level, package-level, and multichip module substrate-level interconnect circuitry based on measured time-domain reflectrometry data. The scattering poles and residues of a multiport system are extracted and used as a model that can be evaluated in linear time by recursive convolution in a SPICE-based simulator. This allows any linear or nonlinear circuits to be connected to the model ports, and the entire circuit may be simulated in a SPICE-based simulagtor. Two-port and four-port example microstrip circuits are characterized, and the simulation results are compared with measured data. Delay, reflection, transmission, and crosstalk are shown to be accurately modeled in each case.**

I. Introduction

As THE RISE times of digital signals drop into the subnanosecond range, the effects of off-chip circuitry become increasingly important. Packaging and board-level circuitry, electrically insignificant at low frequencies, can cause delay, crosstalk, and reflection transients. If not considered during the design stage, these transients can cause logic glitches which render a fabricated digital circuit inoperable, or they can distort an analog signal such that it fails to meet specifications. Since extra iterations in the design cycle of a circuit are costly, accurate prediction of these effects is a necessity.

Interconnect circuitry has traditionally been characterized using models composed of standard linear elements such as resistors, coupled and uncoupled inductors, and capacitors. This approach allows a distributed network to be modeled for a traditional simulator, and if the topology and the element values are well-chosen, the model will accurately represent the actual circuit within a frequency range. For simple circuits with regular geometries, model topology and element values may be determined manually, by inspection or by simple formulas. For more complex circuits, automatic extraction becomes necessary [1], [2], employing methods based on discretization of Maxwell's equations. However, an automatically generated netlist can be prohibitively large, even for a circuit of modest physical size, since the circuit must be discretized into pieces smaller than the smallest propagating wavelength of interest. Strategies have been proposed [3], [4] for reducing a large netlist to an approximate transfer function, if the size of the netlist is manageable. However, adjustment of this type of model to match empirical data is difficult.

Manuscript received February 15, 1995; revised May 25, 1995.

The authors are with the University of Washington at Seattle, Department of Electrical Engineering, Seattle, WA 98195 USA.

IEEE Log Number 9413424.

Coupled and uncoupled transmission line models have been presented as alternatives to lumped-element approximation [5], [6]. These models are generally derived analytically from Maxwell's equations, subject to particular sets of boundary conditions. While they allow efficient simulation of specific distributed geometries without resorting to lumped equivalent circuits, these models are not easily derived for general circuits in which geometry and coupling vary with position in a complicated fashion.

Modeling techniques based on numerical impulse response data have been proposed to simulate circuits whose characteristics are difficult to describe analytically, and circuits for which extraction of lumped representations is difficult or costly. These techniques allow measured or computed impulse response data to be incorporated into the simulation model. Frequency domain approaches [7], [8] are difficult to extend to the case of arbitrary nonlinear loads, although this was accomplished in [9]. Techniques which require full convolution [10]–[12] can be computationally inefficient if the system impulse response waveforms are long. A recursive technique was proposed in [13], but was not verified against measurement.

This paper presents a verifiable approach for modeling interconnect circuits on printed-wire boards, IC packages, or multichip module (MCM) substrates. Dominant scattering poles and residues are extracted from the measured time-domain step response waveforms of a multiport, and are used as model parameters. This approach avoids using large lumped-element equivalent circuits to characterize distributed networks, and can be automated. The model which is presented can be incorporated into a SPICE-based simulator and evaluated in linear time using recursive convolution. Because the parameters are extracted from the measured response, linear circuits with arbitrary geometry and cross-coupling, which are often encountered in interconnects, can be characterized without exact knowledge of their internal characteristics. Two-port and four-port example microstrip circuits are measured, characterized, and simulated. Comparison between simulation results and measurement show that delay, reflection, and crosstalk are accurately modeled by this strategy [14].

II. Model Extraction

In the approach presented in this paper, models are extracted directly from the measured time-domain response of a circuit. Extraction using measured data greatly decouples the modeling process from circuit topology and geometry. Time-domain data is used since it is well suited to analysis of digital

circuits, which is performed primarily in the time domain to observe nonlinear broadband effects. Scattering parameters are employed for model formulation since they are measurable at high frequency, and because a scattering impulse response is typically shorter in duration than its admittance or impedance counterpart. This makes scattering parameters preferable as a tool for describing and working with a nearly lossless network in the time domain, since equivalent information is contained in fewer data points.

A. Impulse Response Approximation

If a causal linear time-invariant network is excited at $t = 0$, the vector of reflected voltage waves $b(t)$ is related to the vector of incident voltage waves $a(t)$ according to

$$b(t) = S(t) \otimes a(t) = \int_0^t S(\tau)a(t-\tau)\,d\tau. \tag{1}$$

Discretizing (1) for use with sampled data results in

$$b[n] = S[n] \otimes a[n] = \sum_{k=0}^{n} S[k]a[n-k]\Delta k. \tag{2}$$

If all incident voltage waves but the one at port j are identically zero, which implies a matched load at every port except j, (2) reduces to the scalar relation

$$\begin{aligned} b_i[n] &= S_{ij}[n] \otimes a_j[n] \\ &= \sum_{k=0}^{n} S_{ij}[k]a_j[n-k]\Delta k \quad (a_m = 0, m \neq j). \end{aligned} \tag{3}$$

Since time-domain reflectometry (TDR) measures the incident voltage wave $a_j[n]$ and the reflected voltage wave $b_i[n]$, each impulse response scattering parameter $S_{ij}[n]$ can be determined by deconvolving a single signal $a_j[n]$ out of $b_i[n]$. Deconvolution in discrete time is the inverse of the operation in (3).

Although deconvolution may theoretically be performed in the sampled time domain or in the sampled frequency domain, neither approach, when applied directly, gives an accurate approximation of the impulse response. This is due to the ill-conditioning of the deconvolution problem [15], which allows measurement noise to dominate the solution. In this work, suboptimal filtering [15] was used to improve the conditioning of deconvolution, according to the relationship

$$S_{ij}(j\Omega) = \frac{\mathrm{FFT}(\mathrm{diff}(b_i[n]))}{\mathrm{FFT}(\mathrm{diff}(a_j[n]))} H(j\Omega). \tag{4}$$

The difference function was applied to each of the signals to obtain a time-limited signal to which the FFT could be applied. The smoothing filter $H(j\Omega)$ is used to window out noise which is introduced at frequencies past the noise threshold of $a_j[n]$. This noise is introduced because both spectra are approximately zero at these frequencies, causing the ratio of the two signals to vary unpredictably. In general $H(j\Omega)$ is a low-pass filter with a cutoff frequency near the noise floor of $a_j[n]$.

Deconvolution was also implemented by discrete differentiation of the TDR step response

$$S_{ij}[n] = \mathrm{diff}(b_i[n]) \tag{5}$$

in some cases where the input rise time was much less than the output rise time, since for these cases the input step $a_j[n]$ approaches an ideal step. Both approaches yield an impulse response approximation whose valid frequency range depends on the following parameters: the frequency content of the input step $a_j[n]$, the frequency response of the measurement system, or the sampling frequency of the acquired waveforms. The most restrictive of these three constraints determines the upper limit of the valid frequency range.

B. Exponential Approximation of Impulse Response

A network of resistors, inductors, capacitors, and coupled inductors can be expressed mathematically as a system of linear constant-coefficient differential equations. Therefore, an element of its scattering impulse response matrix is of the form

$$s(t) = k_0\delta(t) + k_1 e^{p_1 t} + \cdots + k_n e^{p_n t} \ (\mathrm{real}(p) \leq 0) \tag{6}$$

where the k_i and p_i are the residues and poles, respectively, of the network. If n is allowed to approach infinity, (6) can also be the impulse response of a distributed network, since a linear distributed element can be decomposed into infinitesimal linear elements. However, the effect of the function $s(t)$ over a finite frequency range can be approximated by a smaller sum composed of the terms in (6) whose poles lie near the frequencies of interest. Therefore, if $s(t)$ is the time-domain scattering response waveform of a linear, time-invariant (and possibly distributed) network, then its scattering impulse response over a finite frequency range can be accurately modeled by a finite sum of $m \leq n$ exponentials.

Similarly, Prony's method [16], [17] allows an evenly-sampled discrete sequence $s[k]$ to be approximated as samples of a function of the form

$$s(t) = k_1 e^{p_1 t} + k_2 e^{p_2 t} + \cdots + k_{n-1} e^{p_{n-1} t} + k_n e^{p_n t}. \tag{7}$$

After the poles p_i of the function are found by means of a Padé approximation [18] in the z domain, the residues k_i are optimized by linear least squares. Prony's method was used in this work to determine the scattering poles and residues of a circuit from its time-domain scattering impulse response.

One difference between (6) and (7), the absence of $k_0\delta(t)$ in the latter, is trivial because a delta function, which implies unlimited frequency content, will not be encountered in measured data. In reality, the valid bandwidth of the impulse-response approximation is limited as discussed in Section II-A. The other difference, discussed in Section II-C, is that (6) requires that $\mathrm{real}(p) \leq 0$.

C. Asymptotic Stability

The simulation model is composed of equations of the form (7). If it is to be physically meaningful and asymptotically stable, the poles must all have negative real parts. However, Prony's method places no constraints on the poles it extracts,

and may on occasion extract positive poles. Since positive poles are nonphysical and are problematic in transient simulation, they are removed from the set of extracted poles prior to residue optimization. Once the residues corresponding to the negative poles are found, the positive poles are considered to have been extraneous if the fit is sufficient in terms of RMS error. This is often the case, because positive poles modeling a waveform which decays to zero are often of very small magnitude, or scaled by extremely small residues, and therefore have an insignificant effect on the waveform. If the fit is poor, then either the positive poles contributed a necessary component to the waveform, or the pole extraction was poorly conditioned [17], and a new set must be re-extracted under different conditions.

D. Refinement of dc Asymptote

To improve the accuracy of the multiport model it is helpful to ensure that the steady-state scattering parameters match the measured steady-state values. The steady-state scattering step response at a circuit port under matched-load conditions is given by

$$b(t \to \infty) - b(0) = [a(t \to \infty) - a(0)] \int_0^\infty s(t)\, dt \qquad (8)$$

which is the area under the associated impulse response waveform scaled by the magnitude of the input step. However, there is no guarantee that the sum of exponentials chosen as a model to interpolate the sampled impulse response waveform achieves exactly the same steady-state value as the true impulse response of the system when both are integrated. In practice it was observed that the integrals may vary by as much as 5% even if the RMS error between the measured and modeled impulse responses is less than 0.1%. If the area under the modeling impulse response waveform differs significantly from the area under the true impulse response waveform, then the simulated results will not match the measured results at dc. The simulated circuit may appear more or less lossy than the actual circuit, or it may even exhibit a dc gain, which is impossible for a passive circuit.

In order to achieve the correct steady-state response, we must explicitly ensure that the integral of each element of the modeling scattering matrix at dc is close to the integral of the corresponding element of the actual scattering matrix at dc. This effectively matches the zeroth Laplace-domain moment of the model to the measured value of the zeroth moment. Because TDR data provides the scattering *step* response of a system, the steady state ratio of reflected voltage to incident voltage provides a good measure of the zeroth moment of the actual system. Matching the zeroth moment of the model to the measured zeroth moment is achieved numerically during optimization of the residues k_i by including

$$\int_0^\infty \left(\sum_i k_i e^{p_i t} \right) dt = \sum_i \left(-\frac{k_i}{p_i} \right) = \frac{b_{ss}}{a_{ss}} \qquad (9)$$

as part of the least squares formulation, where b_{ss} and a_{ss} are measured steady-state values, and p_i are the extracted poles. Equation (9) is a restatement of (8) in which the integral of the true impulse response of the system has been replaced by the integral of the sum of exponentials that models the impulse response. Additionally, the values of $a(0)$ and $b(0)$ have been set to zero.

Equation (9) matches the model dc response with the measured dc response at minor expense to the high-frequency fit. RMS simulation accuracy is improved, since digital signals consist primarily of rapid transitions between steady-state values. This method ensures that the model is passive at dc by matching its steady-state response to that of the actual circuit which is known to be passive. At the same time, it prevents the model from appearing more or less lossy than the circuit it represents.

III. Simulation Algorithm

If the scattering poles and residues of a network are known, then the response of the network for any excitations and terminations may be simulated. For a SPICE-based simulator, a mapping step is necessary at each timepoint to map scattering parameters into admittance parameters. Previous approaches have introduced negative resistances [11] or current-controlled voltage sources (CCVS) [13] to perform the mapping. Adding a resistance in series with each port node of an n-port element introduces n additional nodes to the circuit matrix. Adding a CCVS in series at each port introduces n nodes and n current variables for a total of $2n$ additional nodes. This section outlines how to perform the mapping algebraically before updating the circuit matrix, which simplifies the algorithm and requires no additional circuit nodes or variables.

It was shown in [19], [20] that if the admittance parameters of a multiport are given by a matrix of weighted sums of exponentials, the discrete convolution relationship

$$i_k = Y \otimes v = \sum_{m=0}^{k} Y_m v_{k-m} (\Delta t)_m \qquad (10)$$

may be reduced to a simple linear update at each timepoint k, such that

$$i_k = G_k v_k + i_{0,k}. \qquad (11)$$

The variables G_k and $i_{0,k}$ represent a time-dependent conductance matrix and an independent current source vector, respectively. They are evaluated at each timepoint based on the system poles and residues, and the voltages at the previous two timepoints. The number of operations required to find G_k and $i_{0,k}$ depends only on the number of terms in the sums of exponentials, so that the convolution can be performed in order k operations, while the general convolution sum may require up to order k^2. Since it is not necessary to store large portions of the past history of the circuit, memory usage is also reduced.

If instead of the admittance parameters we are given the *scattering* parameters of a multiport in terms of sums of exponentials, the convolution relation in (2) may be reduced to a similar linear update at the kth timestep

$$b_k = \Gamma_k a_k + b_{0,k}. \qquad (12)$$

The incident voltage waves a and the reflected voltage waves b are related to the current and voltage according to the relations

$$a = \frac{1}{2}(v + Y_0^{-1} i)$$
$$b = \frac{1}{2}(v - Y_0^{-1} i) \tag{13}$$

where Y_0 is the diagonal characteristic admittance matrix used to normalize the scattering parameters. Substituting (13) into (12) at the kth timestep gives

$$i_k = \underbrace{Y_0(I + \Gamma_k)^{-1}(I - \Gamma_k)}_{G_k} v_k - \underbrace{2Y_0(I + \Gamma_k)^{-1} b_{0,k}}_{-i_{0,k}} \tag{14}$$

where I is the $n \times n$ identity matrix. Comparing (14) with (11) results in

$$G_k = Y_0(I + \Gamma_k)^{-1}(I - \Gamma_k) \tag{15}$$
$$i_{0,k} = -2Y_0(I + \Gamma_k)^{-1} b_{0,k}. \tag{16}$$

This mapping allows the convolution to be performed in linear time given the scattering-parameter poles and residues and the characteristic admittance matrix of the model. The model can be easily implemented in a SPICE-based simulator because it is implemented in the circuit matrix as conductors and current sources.

Because the n conductors and n current sources in (15) and (16) are connected between existing circuit nodes, they introduce no variables to the circuit matrix. This represents a time savings over methods which utilize series resistances or CCVS elements. Although the inversion of an $n \times n$ matrix at each timepoint is implicit in the equations, this matrix is typically much smaller than the $N \times N$ (sparse) matrix which must be inverted, where N is the number of nodes in the entire netlist.

IV. Results

In this section, two example circuits are characterized: the first is a two-port transmission line circuit with a discontinuity. Reflection and transmission are simulated for various terminations and compared with measured results. The second example consists of a pair of tightly-coupled nonuniform microstrip lines. Reflection, transmission, and crosstalk are simulated for various terminations and the results are compared with measured data.

TDR measurements were made with a Tektronix 11801A Digital Sampling Oscilloscope and SD-24 TDR Sampling Head connected to a personal computer. The TDR is connected to the device under test (DUT) by 50 Ω, 2±.02 ns coaxial lines. Model implementation and circuit simulation were performed using MISIM 3.0 [21].

A. Two-Port Microstrip Circuit

The two-port microstrip circuit in Fig. 1 was characterized according to the method presented in Section II of this paper. The circuit consists of two lengths of 50 Ω transmission line connected by a short piece of soldered wire, and has a 50 Ω SMA coaxial connector at each end. The physical length of the circuit is about 14 cm.

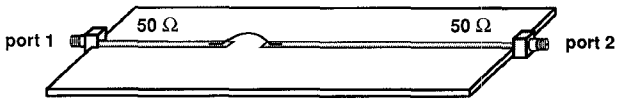

Fig. 1. Two-port microstrip example circuit. The physical distance between ports 1 and 2 is approximately 14 cm.

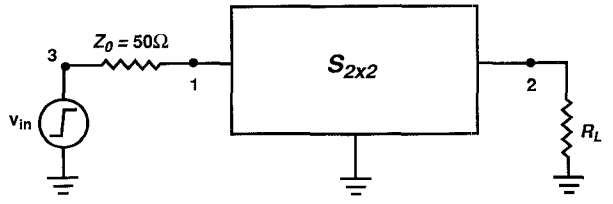

Fig. 2. Circuit used to generate simulation data for comparison with measured data from the two-port circuit in Fig. 1.

To measure the incident step, the DUT was removed from the measurement setup, and the reflection was measured with the 50 Ω cable unterminated. This method provides a good approximation to the incident voltage wave, since $\Gamma \approx 1$ for the unterminated cable at these frequencies.

To compute each impulse response waveform, the incident signal $a_j[n]$ and the reflected signal $b_i[n]$ were differentiated in discrete time to obtain time-limited signals, and deconvolution was performed in the frequency domain by dividing the FFT's of the two signals. The result was transformed back into the time domain by the inverse FFT, and a 10th-order low pass Butterworth filter with $\omega_c = 2 \times 10^{11}$ rad/s was applied to reduce the effect of the ill-conditioning discussed in Section A. Due to the ideal delay present in the system, 36 poles were necessary to represent the reflection waveform at port 1 to within 1% accuracy. The pole-residue pairs of the scattering parameters, together with the characteristic admittance matrix, constitute the model.

In order to evaluate the accuracy of the extracted model of the circuit in Fig. 1, the model was inserted into the circuit shown in Fig. 2 for simulation. Port 1 was driven by a step input through a 50 Ω input resistance, and port 2 was terminated by resistance R_L. Fig. 3(a) compares simulated voltage at port 1 for $R_L = 50$ kΩ with TDR data measured with port 2 unterminated. Fig. 3(b) compares simulated voltage at port 1 for $R_L = 0.001$ Ω with TDR data measured when port 2 was short-circuited. Delay and reflection are accurately modeled in both simulated waveforms, and successive reflections caused by the mismatched load at port 2 are accurately represented. Fig. 3(c) compares simulated transmitted voltage at port 2 for $R_L = 50$ Ω with transmission data measured under the same conditions.

B. Four-Port Microstrip Circuit

The four-port microstrip circuit in Fig. 4 consists of two mirrored striplines of varying width terminated at each end by 50 Ω SMA coaxial connectors. There is no ground plane under the majority of each microstrip run, which allows significant crosstalk between the two lines. The physical length of each run is about 14 cm. Because the slope of the input step

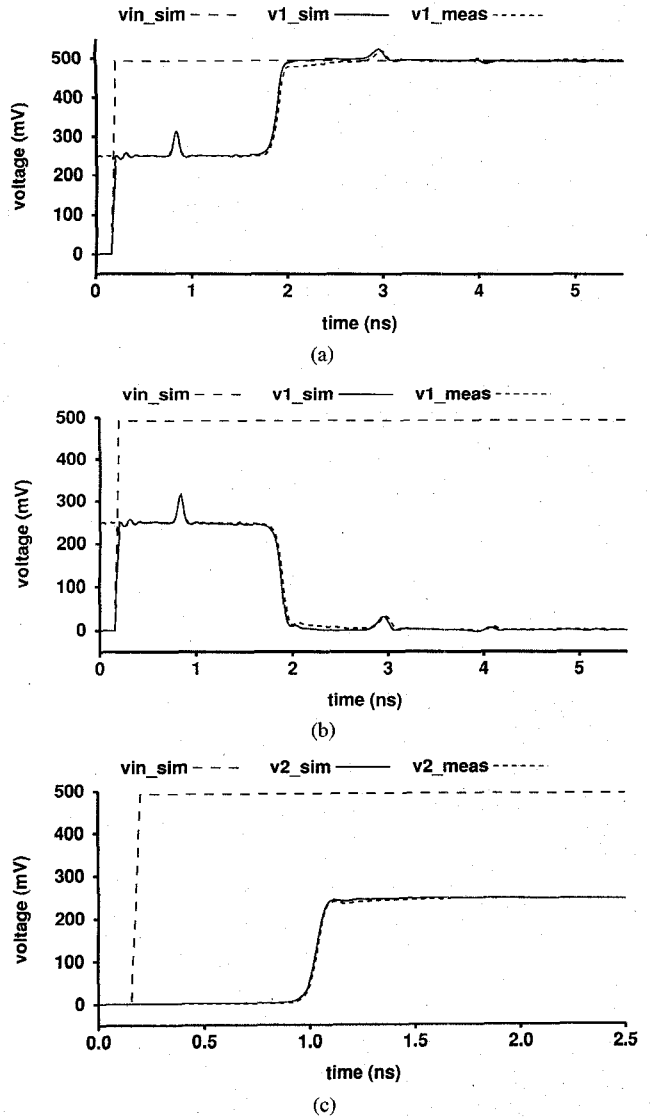

Fig. 3. Comparison of simulated and measured data for circuit in Fig. 1. (a) Open-circuit reflection at port 1. (b) Short-circuit reflection at port 1. (c) Matched-load transmission at port 2.

was steep compared to the response waveform features being modeled, the input step was taken to be an ideal step, and discrete differentiation was used to approximate the impulse response. As shown in Fig. 5, 33 poles were required to capture the detail of the reflection waveform at port 1, although as few as 12 were sufficient to model the major effects. Although the 12-pole response is seen to diverge slightly from the 33-pole response and the measured response, both generated responses converge to zero at dc. The measured reflection converges to a small negative value at dc due to a slightly mismatched load at port 2.

In order to evaluate the accuracy of the extracted model, it was inserted into the circuit shown in Fig. 6. Port 1 was driven by a step input through a 50 Ω input impedance, port 2 was terminated by $R_L = 50$ kΩ, and ports 3 and 4 were terminated by 50 Ω resistors. Fig. 7 compares simulation results for reflection at port 1 and crosstalk at port 4 with measured results for which port 2 was unterminated. The simulated and measured curves are nearly overlapping at the scale shown.

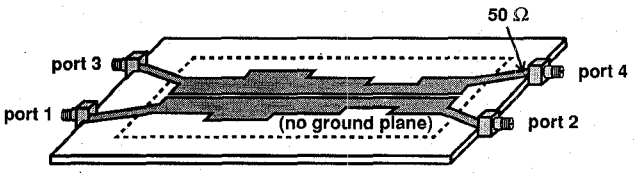

Fig. 4. Four-port microstrip example circuit. The physical distance between ports 1 and 2 is approximately 14 cm.

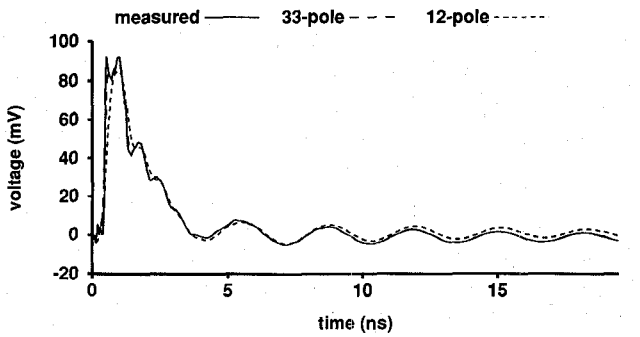

Fig. 5. Comparison of measured $s_{11}(t)$ step response with those generated by direct convolution from 12-pole and 33-pole impulse response approximations.

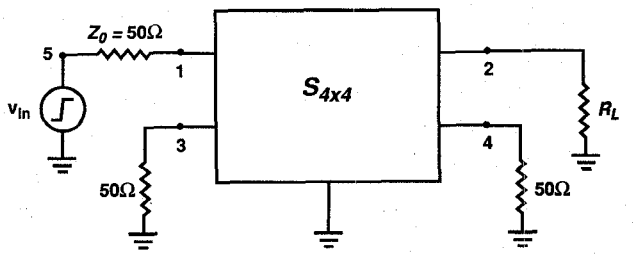

Fig. 6. Circuit used to generate simulation data for comparison with measured data from the four-port circuit in Fig. 4.

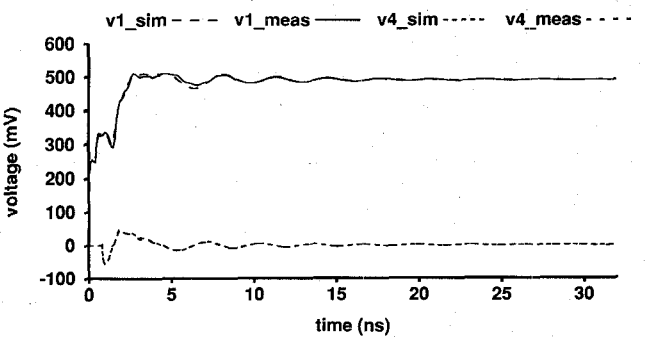

Fig. 7. Open-circuit reflection at port 1 and crosstalk at port 4 for the circuit in Fig. 4.

V. Conclusion

This paper presented a general approach for characterizing interconnect circuitry at the board, package, and MCM substrate levels using measured time-domain data. The technique uses the dominant scattering poles and residues extracted from TDR data as parameters for a circuit model, and can be automated. The model may be implemented in a SPICE-based simulator, and is evaluated in linear time. The approach models delay and reflection introduced by interconnects, as well as crosstalk between multiple conductors of varying geometries,

as accurately as these effects can be measured. As a result, large lumped-element models are not necessary to represent distributed interconnect networks for which time-domain data is available. Two-port and four-port example microstrip circuits were measured, characterized, and simulated, and the results were compared with measured data to demonstrate the validity of the approach.

ACKNOWLEDGMENT

The authors would like to thank the Advanced Laboratory Instruments Test and Measurement group at Tektronix for measurement equipment, test circuits, and helpful suggestions.

REFERENCES

[1] A. Ruehli, "Equivalent circuit models for three dimensional multiconductor systems," *IEEE Tran. Microwave Theory Tech.*, vol. 22, no. 3, pp. 216–224, Mar. 1974.
[2] A. E. Ruehli and H. Heeb, "Circuit models for three-dimensional geometries including dielectrics," *IEEE Trans. Microwave Theory Tech.*, vol. 40, no. 7, pp. 1507–1516, July 1992.
[3] V. Raghavan *et al.*, "AWE-inspired," in *Proc. 1993 IEEE Custom Integrated Circuits Conf.*, May 1993, pp. 18.1.1–18.1.8.
[4] P. Feldmann and R. W. Freund, "Efficient linear circuit analysis by Padé approximation via the Lanczos process," in *Proc. European Design Automation Conf.*, Sept. 1994, pp. 170–175.
[5] F. H. Branin, "Transient analysis of lossless transmission lines," *Proc. IEEE*, vol. 55, no. 11, pp. 2012–2013, Nov. 1967.
[6] F. Y. Chang, "Transient analysis of lossless coupled transmission lines in a nonhomogeneous dielectric medium," *IEEE Trans. Microwave Theory Tech.*, vol. 18, no. 9, pp. 616–626, Sept. 1970.
[7] A. Djordjevic and T. K. Sarkar, "Analysis of time response of lossy multiconductor transmission line networks," *IEEE Trans. Microwave Theory Tech.*, vol. 35, no. 10, pp. 898–908, Oct. 1987.
[8] B. J. Cooke, J. L. Prince, and A. C. Cangellaris, "S-parameter analysis of multiconductor integrated circuit interconnect systems," *IEEE Trans. Computer Aided Design*, vol. 11, no. 3, pp. 353–360, Mar. 1992.
[9] R. Kipp, C. H. Chan, A. T. Yang, and J. T. Yao, "Simulation of high-frequency integrated circuits incorporating full-wave analysis of microstrip discontinuities," *IEEE Trans. Microwave Theory Tech.*, vol. 41, no. 5, pp. 848–854, May 1993.
[10] D. S. Gao, A. T. Yang, and S. M. Kang, "Accurate modeling and simulation of interconnection delay and crosstalks in high-speed integrated circuits," *IEEE Trans. Circuits Syst.– I & II*, vol. 37, no. 1, pp. 1–9, Jan. 1990.
[11] D. Winklestein, M. B. Steer, and R. Pomerleau, "Simulation of arbitrary transmission lines with nonlinear terminations," *IEEE Trans. Circuits Syst.– I & II*, vol. 38, no. 4, pp. 418–422, Apr. 1991.
[12] L. P. Vakanas, A. C. Cangellaris, and O. A. Palusinski, "Scattering parameter-based simulation of transients in lossy nonlinearly-terminated packaging interconnections," *IEEE Trans. Components, Packaging and Manufacturing Technol., Part B: Advanced Packaging*, vol. 17, no. 4, pp. 472–479, Nov. 1994.
[13] G. V. Devarayanadurg and M. Soma, "An interconnect model for arbitrary terminations based on scattering parameters," *Analog Integrated Circuits and Signal Processing*, vol. 5, no. 1, pp. 31–45, Jan. 1994.
[14] S. Corey and A. T. Yang, "Interconnect characterization using time-domain reflectometry," in *Proc. IEEE 3rd Topical Meet. Elec. Perf. Electron. Packaging*, Nov. 1994, pp. 189–191.
[15] E. K. Miller, ed., *Time-Domain Measurements in Electromagnetics*. New York: Van Nostrand-Reinhold, 1986, pp. 87–93.
[16] F. B. Hildebrand, *Introduction to Numerical Analysis*. New York: McGraw-Hill, 1974, pp. 457–462.
[17] D. Tufts and R. Kumaresan, "Estimation of frequencies of multiple sinusoids: Making linear prediction perform like maximum likelihood," *Proc. IEEE*, vol. 70, no. 9, pp. 975–989, Sept. 1982.
[18] G. A. Baker, Jr. and P. Graves-Morris, *Padé Approximants*. New York: Addison-Wesley, 1981.
[19] A. Semlyen and A. Dabuleanu, "Fast and accurate switching transient calculations on transmission lines with ground return using recursive convolutions," *IEEE Trans. Power Apparatus Syst.*, vol. 94, no. 2, pp. 561–571, Mar./Apr. 1975.
[20] V. Raghavan, J. E. Bracken, and R. A. Rohrer, "AWESpice: A general tool for the accurate and efficient simulation of interconnect problems," in *Proc. 29th ACM/IEEE Des. Automat. Conf.*, June 1992, pp. 87–92.
[21] J. T. Yao and A. T. Yang, "Consistent nonlinear analysis based on improved harmonic balance techniques," in *Proc. 1993 European Design Automation Conf.*, Sept. 1993, pp. 430–435.

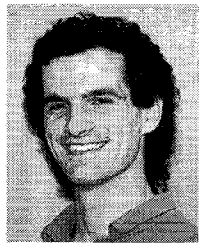

Steven D. Corey received the B.S. and M.S. degrees in electrical engineering from the University of Washington in Seattle in 1991 and 1994, respectively. He is currently working toward the Ph.D. degree at the University of Washington.

He spent the summer of 1994 working on package modeling and measurement at Tektronix. His research interests include numerical methods, simulation and modeling of linear interconnect, and linear network reduction.

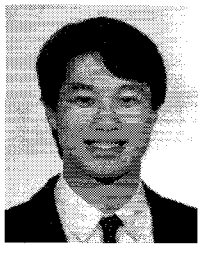

Andrew T. Yang received the B.S. degree in electrical engineering and computer science from the University of California at Berkeley in 1983, and the M.S. and Ph.D. degrees from the University of Illinois at Urbana-Champaign in 1986 and 1989, respectively.

From 1983 to 1984, he was with the Advanced Micro Device Corporation, CA. Since 1989 he has been with the University of Washington at Seattle where he is currently an Associate Professor of Electrical Engineering. His current research interests include simulation of mixed analog-digital circuits, timing simulation with emphasis on analog modeling, and modeling of semiconductor devices.

Dr. Yang has served as a member of the technical program committee of the IEEE International Conference on Computer-Aided Design. In 1992, he received the NSF Young Investigator Award.